

Figure S1. IKK α Supports Autophagosome-Lysosome Fusion to Control Autophagic Flux, Related to Figure 1

(A) IB analysis showing the free GFP fragment in GFP-LC3 expressing parental (WT) and IKK α -KD MIA PaCa-2 cells incubated in normal or glucose (Glu)-free medium for 4 hrs.

(B) Imaging and quantification of LC3 puncta in WT and IKK α -KD MIA PaCa-2 cells incubated in normal or starvation (starv.) medium for 2 hrs. Scale bar, 20 μ m.

(C) IB analysis of p62 and LC3 in WT and IKK α KD MIA PaCa-2 cells incubated in normal or starvation medium for 2 hrs +/- CQ. The LC3II/ β -actin and p62/ β -actin ratios were determined by Image J analysis.

(D) IB analysis of human PDAC patient derived xenografts (PDXs) with high and low IKK α expression.

(E) IB analysis of IKK α ^{high} (1444) and IKK α ^{low} (1305, 1334) human primary PDAC cells derived from above PDXs.

(F) Imaging of LC3 puncta and NRF2 in IKK α ^{high} and IKK α ^{low} cells. LC3 puncta (n = 30 cells) and NRF2 (n = 6 fields) nuclear localization were quantified (shown on the right). Scale bar 10 μ m.

(G) IB analysis showing the free GFP fragment generated in GFP-LC3 transfected 1444 and 1334 cells incubated in normal or Glu-free medium for 4 hrs. The GFP/HSP90 ratio was determined by Image J analysis.

(H) IB analysis of p62 and LC3 in 1334 cells +/- OE IKK α incubated in normal or starvation medium for 2 hrs.

(I) Imaging and quantification (on the right) of LC3 puncta in above cells. Scale bar, 10 μ m.

(J) IB analysis of p62 and LC3 in WT and IKK α^{Δ} 1444 cells incubated in normal or starvation medium for 2 hrs +/- CQ.

(K) Imaging and quantification of GFP-LC3 and LAMP1 co-localization in GFP-LC3-stable WT and IKK α -KD MIA PaCa-2 cells incubated in starvation medium for 2 hrs. Co-localization coefficients are presented to the right as the percentage of GFP-LC3 puncta positive for LAMP1.

Scale bar, 10 μ m.

Results in (B), (I) and (K) are mean \pm SEM (n=30). Statistical significance was determined by a 2-tailed t-test. *p < 0.05, **p < 0.01, ***p < 0.001, ****p < 0.0001.

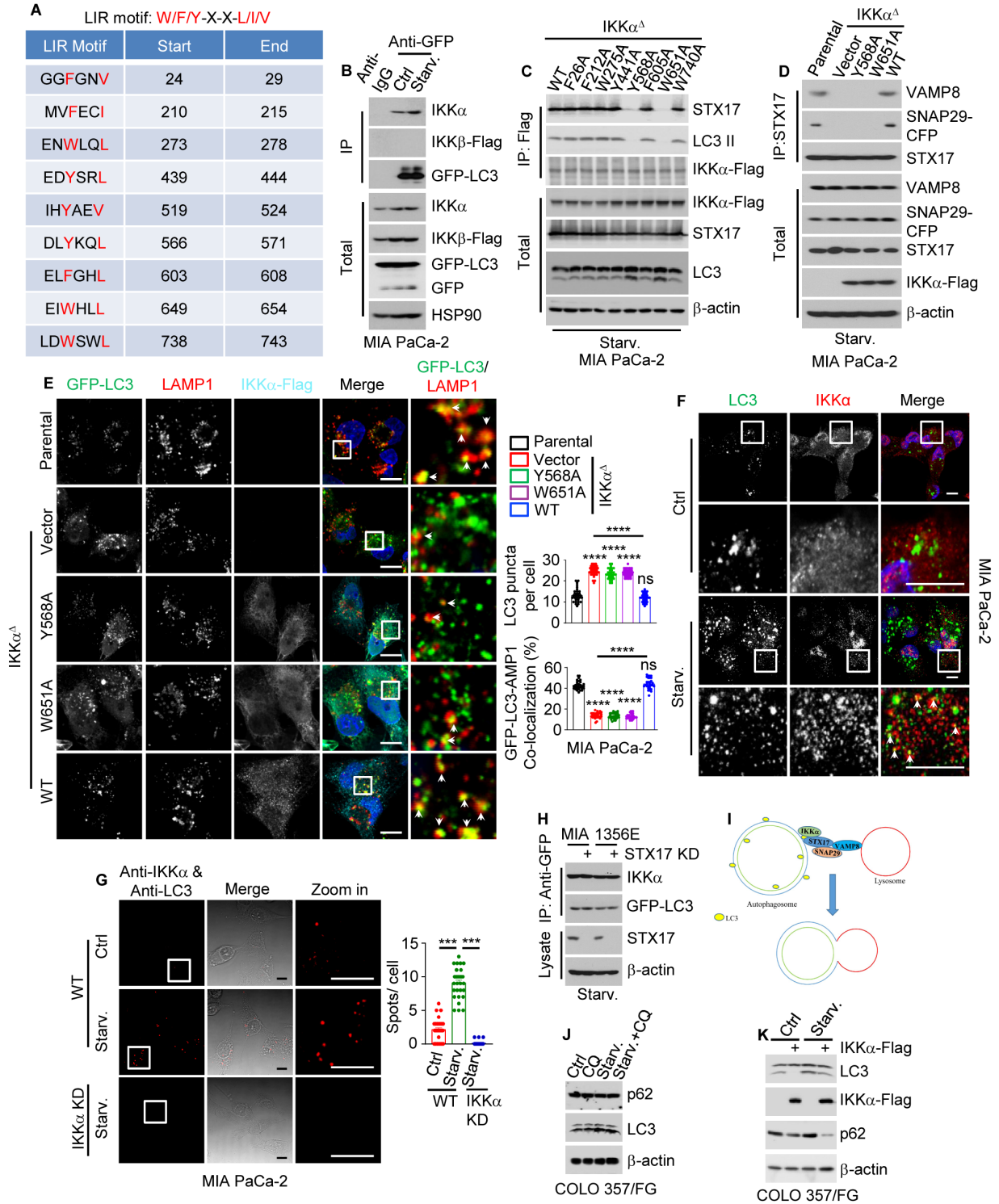


Figure S2. IKK α Binds LC3 to Enhance Autophagic Flux, Related to Figure 1

(A) LC3 interaction (LIR) motifs in human IKK α .

(B) Co-IP of IKK α , IKK β -Flag with GFP-LC3 in co-transfected MIA PaCa-2 cells incubated +/- starvation medium for 2 hrs.

(C) Co-IP of STX17, LC3 with Flag-tagged WT and LIR-mutated IKK α in IKK α^{Δ} MIA PaCa-2 cells incubated in starvation medium for 2 hrs.

(D) Co-IP of VAMP8, SNAP29-CFP with STX17 in starved WT and IKK α^{Δ} MIA PaCa-2 cells transiently co-transfected with vector control, WT or LIR-mutated IKK α variants .

(E) Imaging and quantification of GFP-LC3 puncta and GFP-LC3 and LAMP1 co-localization in GFP-LC3-stable WT and IKK α^{Δ} MIA PaCa-2 cells treated as above. Co-localization coefficients are presented on the right as the percentage of GFP-LC3 puncta positive for LAMP1. Mean \pm SEM (n=30). Statistical significance was determined by a 2-tailed t-test. ****p < 0.0001. Scale bar, 10 μ m.

(F) Co-localization of LC3 and IKK α in MIA PaCa-2 cells incubated in normal or starvation medium for 2 hrs. Scale bar, 10 μ m.

(G) Representative images and quantification (on the right) of proximity ligated (red) IKK α and LC3. Mean \pm SEM (n=30). Statistical significance was determined by a 2-tailed t-test; ***p < 0.001. Scale bar, 10 μ m.

(H) Co-IP of IKK α with GFP-LC3 in WT and STX17 KD MIA PaCa-2 (MIA) or 1356E cells incubated in starvation medium for 2 hrs.

(I) Proposed mechanism of IKK α -enhanced autophagosome-lysosome fusion.

(J, K) IB analysis of p62 and LC3 in COLO 357/FG cells +/- IKK α transfection incubated in normal or starvation medium for 2 hrs +/- CQ.

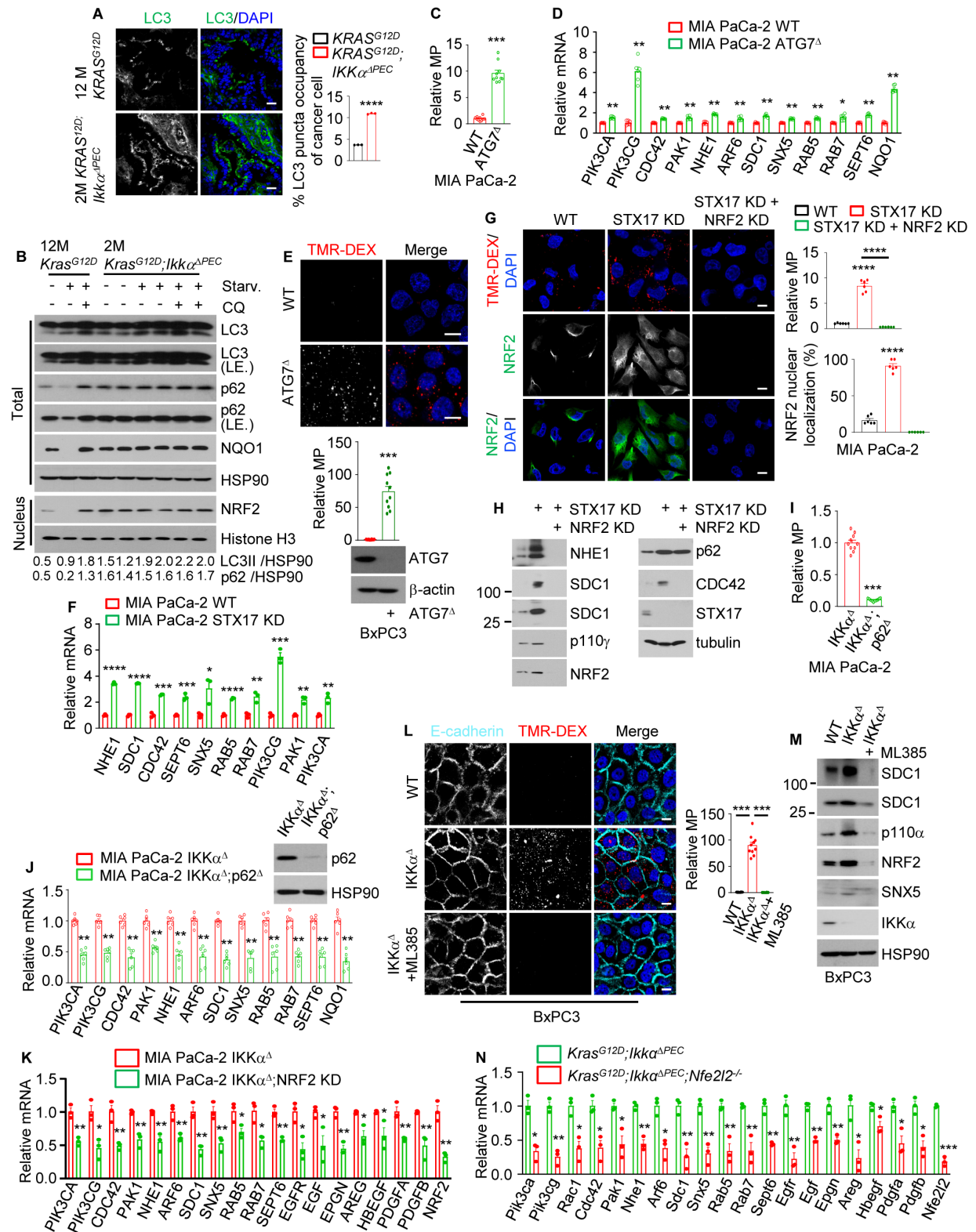


Figure S3. ATG7, STX17 or IKK α Ablations Upregulate MP via the p62-NRF2 Axis,

Related to Figure 3

- (A) Imaging and quantification of LC3 puncta in pancreata of the indicated mice, which were starved for 36 hrs prior to the analysis. Scale bar, 10 μ m.
- (B) IB analysis of the denoted proteins in PEC isolated from the indicated mice, which were starved for 36 hrs and were either injected or not with CQ.
- (C) Quantification of MP using TMR-DEX in WT and ATG7 Δ MIA PaCa-2 cells.
- (D) qRT-PCR analysis of MP-related mRNAs in WT and ATG7 Δ MIA PaCa-2 cells.
- (E) MP visualization and quantification using TMR-DEX and ATG7 IB in parental and ATG7 Δ BxPC3 cells. Scale bar, 10 μ m.
- (F) qRT-PCR analysis of MP-related mRNAs in WT and STX17 KD MIA PaCa-2 cells.
- (G) Imaging and quantification of MP using TMR-DEX and NRF2 nuclear localization in WT, STX 17 KD and STX 17;NRF2 double KD cells. Scale bar, 10 μ m.
- (H) IB analysis of MP-related proteins in above cells.
- (I) Quantification of MP using TMR-DEX in IKK α Δ and IKK α Δ ;p62 Δ (DKO) MIA PaCa-2 cells.
- (J) qRT-PCR analysis of MP-related mRNAs and p62 IB in above cells.
- (K) qRT-PCR analysis of MP-related mRNAs in IKK α Δ and IKK α Δ ;NRF2 KD MIA PaCa-2 cells.
- (L) MP visualization and quantification in WT and IKK α Δ BxPC3 cells treated +/- the NRF2 inhibitor ML385 (10 μ M) for 24 hrs. Scale bar, 10 μ m.
- (M) IB analysis of indicated proteins in above cells.
- (N) qRT-PCR analysis of MP-related mRNAs in PEC isolated from 3-mo mice of indicated genotypes.

Results in (A) (n=3), (C), (E), (I) and (L) (n=10), (D), (G) and (J) (n=6) and (F), (K) and (N) (n=3) are mean \pm SEM. Statistical significance was determined by a 2-tailed t-test. *p < 0.05, **p < 0.01, ***p < 0.001, ****p < 0.0001.

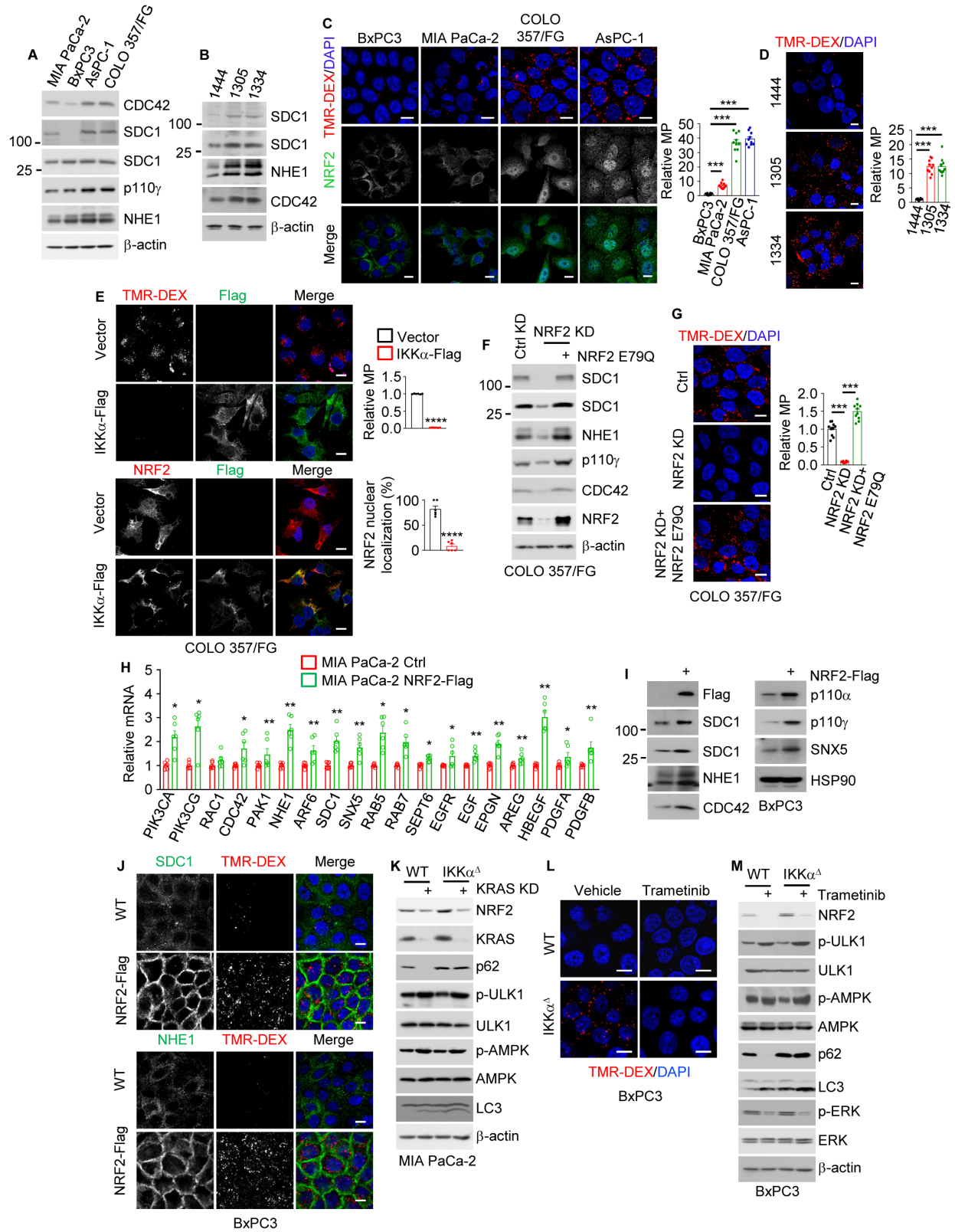


Figure S4. NRF2 Stimulates MP, Related to Figure 3

(A, B) IB analysis of MP-related proteins in established human PDAC cell lines (A) and primary cells (B).

(C) Macropinosome and NRF2 localization in indicated human PDAC cell lines. MP activity was quantified and shown on the right.

(D) MP visualization and quantification using TMR-DEX in primary human PDAC cells.

(E) Imaging and quantification of MP using TMR-DEX and NRF2 nuclear localization in COLO 357/FG cells +/- transfected IKK α .

(F) IB analysis of MP-related proteins in WT and NRF2-KD COLO 357/FG cells +/- transfected NRF2(E79Q).

(G) MP visualization and quantification using TMR-DEX in above cells.

(H) qRT-PCR analysis of MP-related mRNAs in MIA PaCa-2 cells +/- transfected NRF2-Flag.

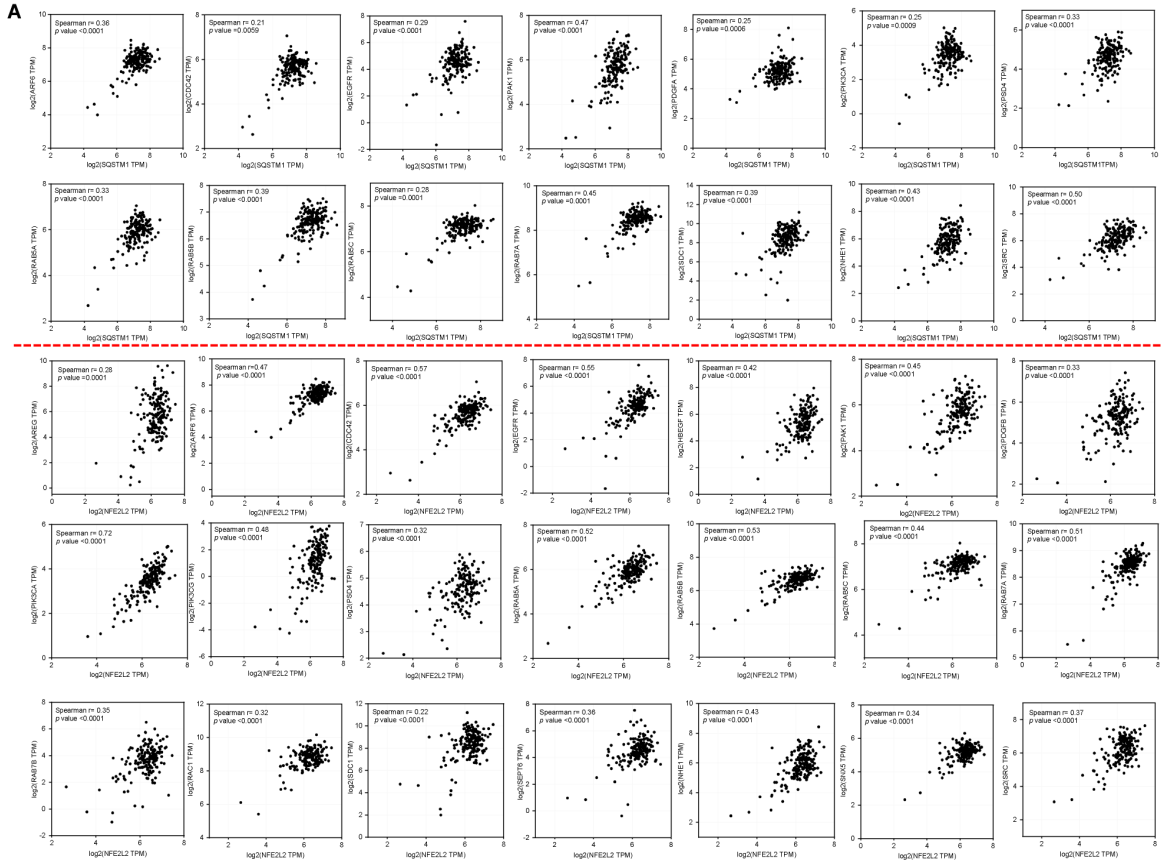
(I) IB analysis of MP-related proteins in BxPC3 cells +/- transfected NRF2-Flag.

(J) Macropinosomes and SDC1 and NHE1 localization in above cells. Scale bar, 10 μ m.

(K) IB analysis of indicated proteins in WT and IKK α^{Δ} MIA PaCa-2 cells +/- KRAS KD.

(L, M) Imaging of macropinosomes (L) and IB analysis of indicated proteins (M) in WT and IKK α^{Δ} BxPC3 cells treated +/- the MEK inhibitor trametinib.

Results in (C), (D) and (G) (n=10), (E) and (H) (n=6) are mean \pm SEM. Statistical significance was determined by a 2-tailed t-test. *p < 0.05, **p < 0.01, ***p < 0.001, ****p < 0.0001. Scale bar, 10 μ m.



B

	Low		High	
	Negative	Weak	Intermediate	Strong
IKK α	6/100	25/100	60/100	9/100
p62	6/100	39/100	9/100	46/100
NRF2	5/100	35/100	10/100	50/100
NQO1	3/100	37/100	15/100	45/100
CDC42	8/100	37/100	20/100	35/100
NHE1	10/100	38/100	15/100	37/100
SDC1	11/100	35/100	11/100	43/100

D

Gene	NRF2 binding sites	Gene	NRF2 binding sites
PIK3CG	-509, -105, 80	NHE1	-85, -523, -756
SNX5	-30, -960, -968	EGF	-574, -20
CDC42	-911, -705	PDGFB	-436, -464, -880
PAK1	-548, -755	SDC1	39, -590, -755

C CDC42 Chi-square test $p=0.004$ **

	CDC42 low	CDC42 high	Total
IKK α low/p62 high/NRF2 high	5	20	25
Others	40	35	75
Total	45	55	100

SDC1 Chi-square test $p=0.011$ *

	SDC1 low	SDC1 high	Total
IKK α low/p62 high/NRF2 high	6	19	25
Others	40	35	75
Total	46	54	100

NHE1 Chi-square test $p=0.006$ **

	NHE1 low	NHE1 high	Total
IKK α low/p62 high/NRF2 high	6	19	25
Others	42	33	75
Total	48	52	100

Figure S5. MP-Related Gene Expression in Human PDAC Correlates with IKK α , p62 and NRF2 Expression, Related to Figure 4

(A) Correlation scatter plots between MP-related and *SQSTM1* or *NFE2L2* mRNAs. The p values and Spearman correlation coefficient (r) are indicated. mRNA expression data were procured from TCGA.

(B) A table depicting the numbers and percentages of human PDAC tissues (n=100) positive for the indicated proteins (arbitrarily indicated as negative, weak, intermediate or strong).

(C) A human PDAC tissue array was IHC-analyzed for IKK α , p62, NRF2 and MP-related proteins in parallel sections. The correlation between MP proteins (CDC42, SDC1 and NHE1) and the IKK α /p62/NRF2 status was analyzed by a Chi-square test. *p < 0.05, **p < 0.01.

(D) Locations of potential NRF2 binding sites relative to the transcriptional start site (TSS, +1) in the indicated MP-related human genes.

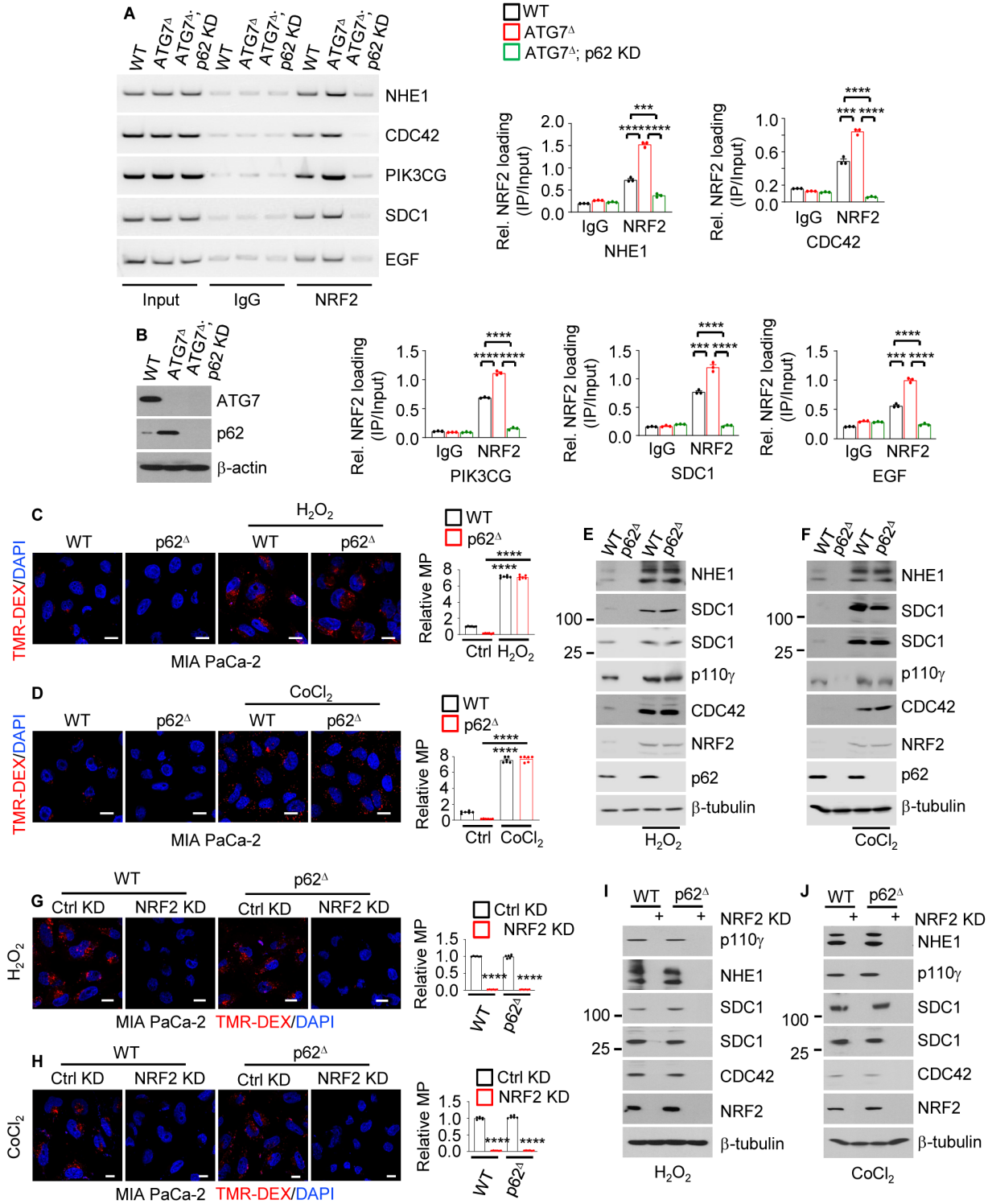


Figure S6. NRF2 Controls MP in Response to Autophagy Deficiency, Oxidative Stress and Hypoxia, Related to Figure 5

(A) ChIP assays probing NRF2 recruitment to the NHE1, CDC42, PIK3CG, SDC1, and EGF promoters in WT, ATG7^Δ and ATG7^Δ;p62 KD MIA PaCa-2 cells. The image shows PCR-amplified promoter DNA fragments containing NRF2 binding sites (AREs). The quantitation is shown to the right.

(B) IB analysis of ATG7 and p62 in above cells.

(C, D) MP visualization and quantification using TMR-DEX in WT and p62^Δ MIA PaCa-2 cells treated +/- H₂O₂ (C) or CoCl₂ (D).

(E, F) IB analysis of MP-related proteins in above cells.

(G, H) MP visualization and quantification using TMR-DEX in WT and p62^Δ MIA PaCa-2 cells +/- NRF2 treated with H₂O₂ (G) or CoCl₂ (H).

(I, J) IB analysis of MP-related proteins in above cells.

Results in (A) (n=3), (C), (D), (G) and (H) (n=6) are mean ± SEM. Statistical significance was determined by a 2-tailed t-test. ***p < 0.001, ****p < 0.0001. Scale bar, 10 μm.

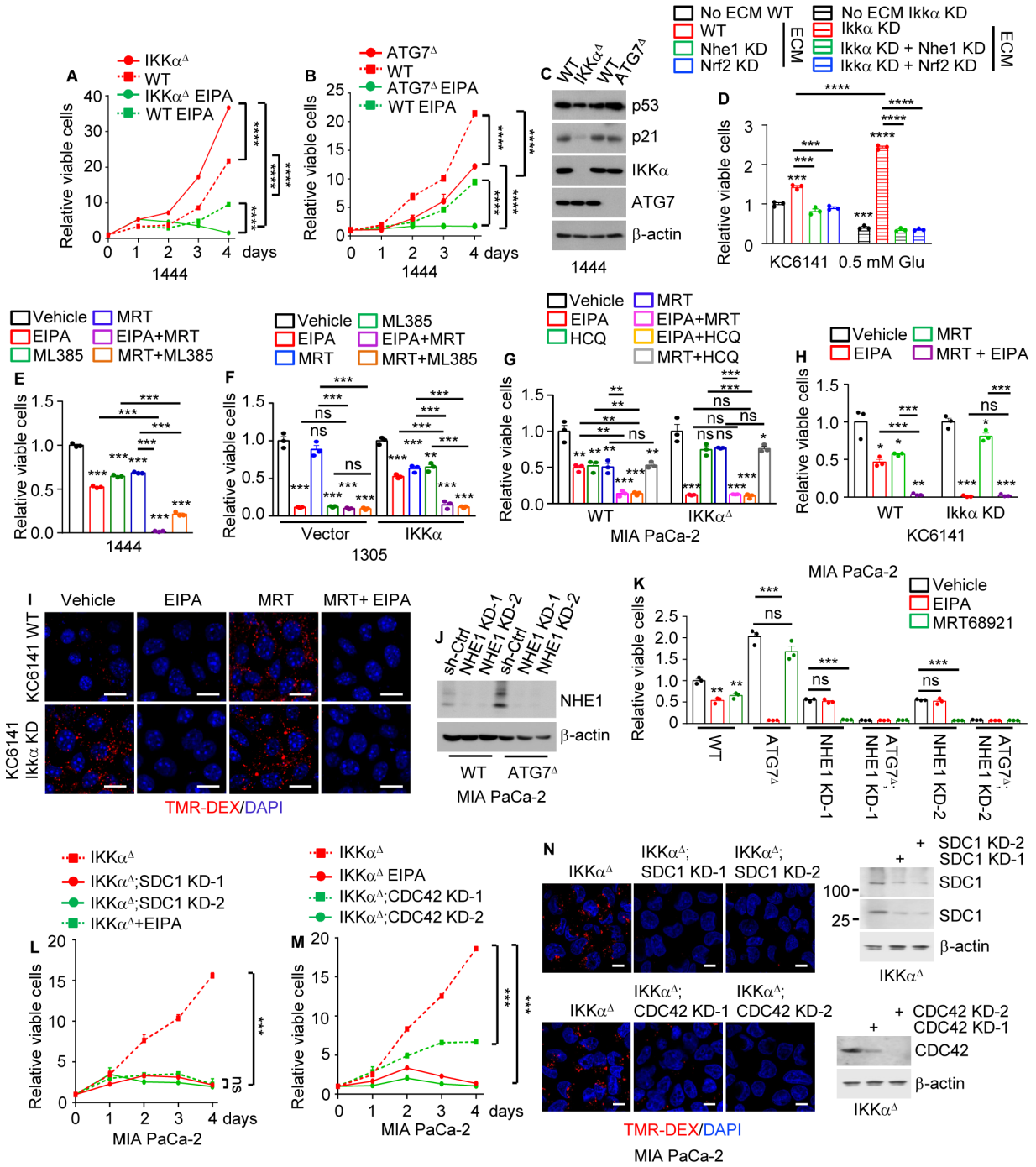


Figure S7. Effects of Autophagy and MP Inhibitors on PDAC Cell Growth, Related to

Figure 6

(A, B) WT and IKK α ^Δ (A) or ATG7^Δ (B) 1444 cells were cultured in complete medium +/- EIPA (10.5 μ M) and total viable cells were measured with the CCK-8 assay after 0, 1, 2, 3 and 4 days. Data are presented relative to the day 0 value.

(C) IB analysis of the indicated proteins in above cells.

(D) The indicated KC6141 cells were grown on plates +/- ECM coating in the presence of 0.5 mM Glu. Total viable cells were measured after 3 days and data are presented relative to the value of WT cells grown without ECM.

(E) 1444 cells were treated with the indicated compounds and total viable cells were measured after 3 days and data are presented relative to the vehicle control value.

(F) WT and IKK α transfected 1305 cells were treated as above and total viable cells were measured as above.

(G) WT and IKK α ^Δ MIA PaCa-2 cells were treated with the indicated compounds and total viable cells were measured as above.

(H) WT and IKK α -KD KC6141 cells were treated with the indicated compounds and total viable cells were measured as above.

(I) Imaging of macropinosomes in WT and IKK α -KD KC6141 cells treated with the indicated compounds. Scale bar, 10 μ m.

(J) IB analysis of NHE1 KD in WT and ATG7^Δ MIA PaCa-2 cells.

(K) The above cells were treated with indicated compounds and total viable cells were measured after 3 days and data are presented relative to the vehicle control values of WT cells.

(L, M) SDC1 (L) or CDC42 (M) KD IKK α ^Δ MIA PaCa-2 cells were treated +/- EIPA and total viable cells were measured as in (A).

(N) Imaging of macropinosomes and IB analysis of SDC1 or CDC42 in above cells. Scale bar, 10 μ m.

Results in (A), (B), (D-H) and (K-M) are mean \pm SEM (n=3 independent experiments).

Statistical significance was determined by a 2-tailed t-test. *p < 0.05, **p < 0.01, ***p < 0.001,

****p < 0.0001.

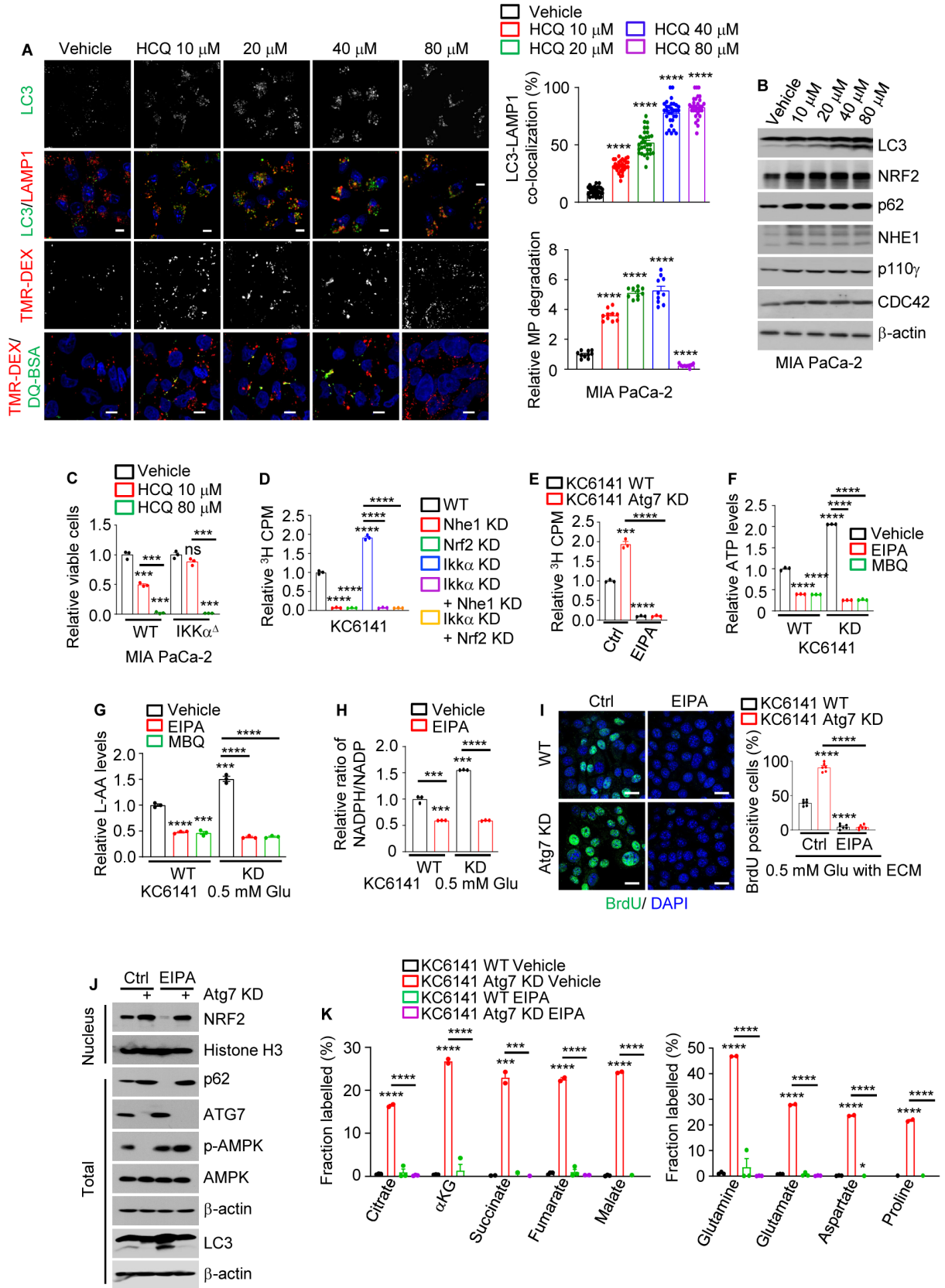


Figure S8. Effect of Autophagy and MP Blockade on PDAC Cell Growth and Metabolism, Related to Figure 7

(A) Imaging and quantification (on the right) of LC3-LAMP1 or TMR-DEX-DQ-BSA co-localization in MIA PaCa-2 cells treated with the indicated concentrations of HCQ.

(B) IB analysis of the indicated proteins in MIA PaCa-2 cells treated as above.

(C) WT and IKK α^{Δ} MIA PaCa-2 cells were treated +/- 10 or 80 μ M HCQ. Total viable cells were measured after 3 days and data are presented relative to the vehicle value. Mean \pm SEM (n=3 independent experiments).

(D, E) The indicated KC6141 cell variants were grown on plates coated with 3 H-proline-labeled ECM in the presence of 0.5 mM Glu +/- EIPA for 24 hrs. 3 H uptake was measured by liquid scintillation counting and the data were normalized to cell number and presented as 3 H CPM relative to WT cells. Mean \pm SEM (n=3 independent experiments).

(F) WT and IKK α -KD KC6141 cells were grown on plates coated with ECM in the presence of 0.5 mM Glu +/- EIPA or MBQ-167 (MBQ) for 24 hrs. Total cellular ATP was measured and data were normalized to cell number and presented relative to untreated WT cells. Mean \pm SEM (n=3 independent experiments).

(G) Total L-amino acids (AA) were measured in WT and IKK α -KD KC6141 cells cultured and treated as above and data were normalized and presented as above. Mean \pm SEM (n=3 independent experiments).

(H) WT and IKK α -KD KC6141 cells were grown as above in the presence of 0.5 mM Glu +/- EIPA for 24 hrs. NADPH and NADP were measured and data were normalized to cell number and presented as NADPH to NADP ratio relative to the value of untreated WT cells. Mean \pm SEM (n=3 independent experiments).

(I) BrdU visualization and quantification in the indicated KC6141 cells grown on plates coated with ECM in the presence of 0.5 mM Glu and 0.5 mg/ml BrdU +/- EIPA for 24 hrs. Scale bar, 10 μ m. Mean \pm SEM (n=6 fields).

(J) IB analysis of the indicated proteins in above cells.

(K) Fractional labeling (mole percent enrichment) of TCA cycle intermediates and intracellular AA in WT and ATG7-KD KC6141 cells cultured for 24 hrs in 0.5 mM Glu medium +/- EIPA on ECM deposited by fibroblasts that were cultured with U-¹³C-glutamine for 6 days.

Statistical significance in (A), (C-I) and (K) was determined by a 2-tailed t-test. *p < 0.05, ***p < 0.001, ****p < 0.0001.

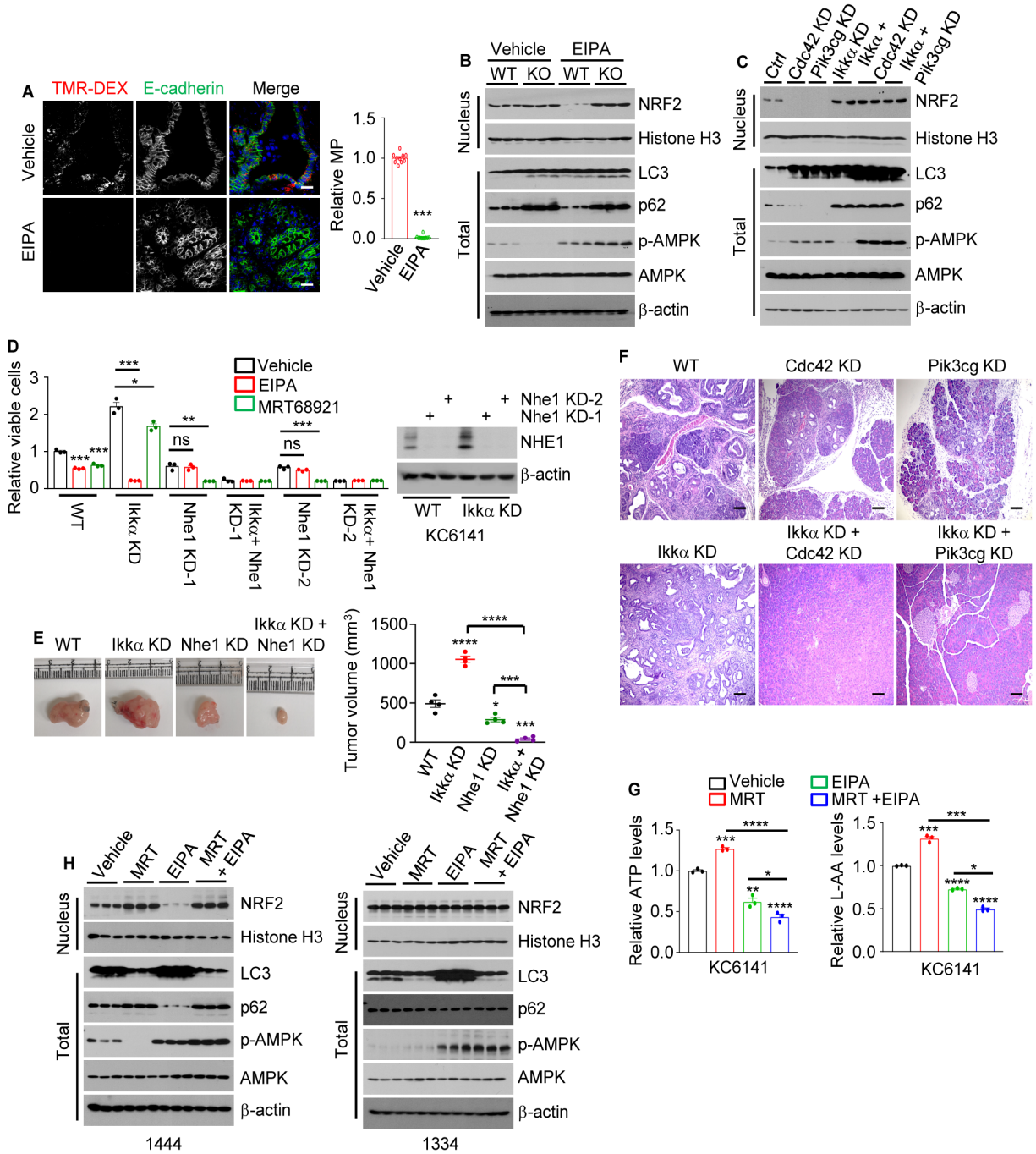


Figure S9. Effect of Autophagy and MP Inhibition on Tumor Development, Autophagy Status and Metabolism, Related to Figure 7

(A) Images and quantification of MP in TMR-DEX injected pancreata from 8-week *Kras^{G12D};Ikkα^{APEC}* mice treated with vehicle or 10 mg/kg EIPA for 1 month. PDAC and PanIN cells are marked by E-cadherin staining. Scale bar, 20 μm. Mean ± SEM (n=10).

(B) IB analysis of indicated proteins in MIA PaCa-2 s.c. tumors grown in nude mice treated with EIPA or vehicle for 5 days prior to harvesting.

(C) IB analysis of the indicated proteins in orthotopic tumors generated by transplantation of the indicated KC6141 cell variants into C57BL/6 mice.

(D) WT and IKKα-KD +/- NHE1-KD KC6141 cells were treated with the indicated compounds. Total viable cells were measured after 3 days and data are presented relative to the vehicle control values of WT cells. Mean ± SEM (n=3 independent experiments). IB analysis of NHE1 is shown on the right.

(E) Representative images and sizes of dissected s.c. tumors generated by WT, IKKα and or NHE1 KD KC6141 cells in C57BL/6 mice. Mean ± SEM (n=4).

(F) H&E-stained pancreatic sections from C57BL/6 mice orthotopically transplanted with the indicated KC6141 cells. Scale bars, 100 μm.

(G) Total cellular ATP and L-AA were measured in tumor cells generated by KC6141 cells in C57BL/6 mice treated with vehicle, EIPA, MRT68921 or MRT68921 + EIPA.

(H) IB analysis of indicated proteins in s.c. 1444 or 1334 tumors grown in nude mice treated with the indicated compounds for 5 days prior to harvesting.

Statistical significance in (A), (D), (E) and (G) was determined by a 2-tailed t-test. *p < 0.05, **p < 0.01, ***p < 0.001, ****p < 0.0001.